Electronic Supplementary Information

A Fluorinated Binaphthyl Chiral Dopant for Fluorinated Liquid Crystal Blue Phases

K. Kakisaka,[a] H. Higuchi,[b] Y. Okumura[b] and H. Kikuchi*[b]

[a] Interdisciplinary Graduate School of Engineering Sciences, Kyushu University, 6-1 Kasuga-Koen, Kasuga, Fukuoka, 816-8580, Japan.

[b] Institute for Material Chemistry and Engineering, Kyushu University, 6-1 Kasuga-Koen, Kasuga, Fukuoka, 816-8580, Japan. E-mail: kikuchi@cm.kyushu-u.ac.jp

This Electronic Supplementary Information contains:

1. Syntheses and Measurements

1.1 Materials and General Methods

Racemic 6,6'-difluoro-2,2'-hydroxy-1,1'-binaphthalene, which is precursor of racemic substance *rac*-**1**, was prepared from racemic BINOL in a similar scheme of the synthesis of (*R*)-**1**.[1-3] Reagents and solvents were purchased from Wako Pure Chemical Industries, Ltd., Tokyo Chemical Industry Co., Ltd., and Kanto Chemical Co., Inc. and used without purification. Thin layer chromatography was conducted on SiO_2-layered grass plate (60 F254; Merck); visualization with UV light (254 or 365 nm). The chromatographic separations were carried out on SiO_2 60 N (particle size 0.063-0.210 mm; Kanto Chemical Co., Inc.). ^{1}H and ^{13}C NMR spectra were measured on JEOL JNM-LA400 (400 MHz) and JEOL ECA-600 (600 MHz) using $CDCl_3$ as a solvent at 25 °C. Chemical shifts are reported in ppm relative to the signal of tetramethylsilane. Residual solvent signals in the ^{1}H and ^{13}C NMR spectra were used as an internal reference. Differential scanning calorimetry measurements were performed on Mettler-Toledo DSC1 at a scanning rate of 5 ºC/min. The melting points were taken at the onset of the phase transition peaks from crystal to isotropic phase at the heating process. Elemental analyses were performed at Kyushu University.

As a host nematic LC, commercial fluorinated nematic LC mixture, JC-1041XX (JNC Co. Ltd., Δn = 0.142, $\Delta\varepsilon$ = 5.7 at 25 ºC), was used. A conventional chiral dopant ISO-(6OBA)$_2$ was synthesized by our laboratory. To determine phase transition temperatures, optical textures were observed under crossed Nicols with Nikon ECLIPSE E600 POL optical microscope and reflectance spectra were measured with UV-Vis micro-spectrometer JASCO MSV-350. The temperatures of the sample were precisely controlled by hot stage (Linkam, LTS-E350), which is controlled by a controller (Linkam, 10013L). The heating rate of the LC samples was 0.5 ºC/min. A glass sandwiched cell without surface alignment and a glass sandwiched cell with ITO square electrode of 1 cm^2 and an antiparallel alignment (cell gap = 10 μm, E. H. C. Co.) are used for the polarizing optical microscopy observation, the reflectance spectrometry, and measurements of elastic constants, respectively.

1.2 Synthesis of Fluorinated binaphthyl Derivative

*1.2.1 Synthesis of racemic 6,6'-difluoro-2,2'-(1,4-butylenedioxy)-1,1'-binaphthalene (rac-**1**)*

A mixture of racemic 6,6'-difluoro-2,2'-dihydroxy-1,1'-binaphthalene (0.11 g, 0.27 mmol), K_2CO_3 (0.087 g, 0.63 mmol), and a catalytic amount of 18-crown-6 in acetone (30 mL) was refluxed for 2 h. 1, 4-dibromobutane (0.066 g, 0.31 mmol) in acetone (5.0 mL) was added dropwise to the solution over 8 hour at reflux temperature, and then the reaction mixture was refluxed for 25 h. After 25 h, excess K_2CO_3 was filtered off. The solution was condensed under reduced pressure and extract with Et_2O. The extract was dried with $MgSO_4$ and evaporated the solvent. The pure *rac*-**1** was obtained after silica gel column chromatography (AcOEt/*n*-heptane = 1:3) and recrystallization from CH_2Cl_2/*n*-heptane in 73% yield.

^1H NMR (400 MHz, $CDCl_3$): δ = 7.89 (d, J = 8.9 Hz, 2H; Ar-H), 7.52 (d, J = 8.9 Hz, 2H; Ar-H), 7.48 (dd, J = 9.6, 2.7 Hz, 2H; Ar-H), 7.05-6.97 (m, 4H; Ar-H), 4.52-4.49 (m, 2H; OCH_2), 4.12 (t, J =11 Hz, 2H; OCH_2) 1.83-1.75 ppm (m, 4H; CH_2); ^{13}C NMR (150 MHz, $CDCl_3$): δ = 159.7 (d, J = 244.2 Hz; CF, naphthalene) 152.8 (d, J = 2.9 Hz; naphthalene) 131.0 (s; naphthalene) 130.4 (d, J = 8.7 Hz; naphthalene) 128.8 (d, J = 4.3 Hz; naphthalene) 128.0 (d, J = 7.2 Hz; naphthalene) 122.4 (s; naphthalene) 118.7 (s; naphthalene) 116.7 (d, J = 24.6 Hz; naphthalene) 111.0 (d, J = 20.2 Hz; naphthalene) 70.5 (s; OCH_2) 25.2 ppm (s; CH_2); elemental analysis calcd (%) for $C_{24}H_{18}F_2O_2$: C 76.58, H 4.82; found: C 76.90, H 4.83.
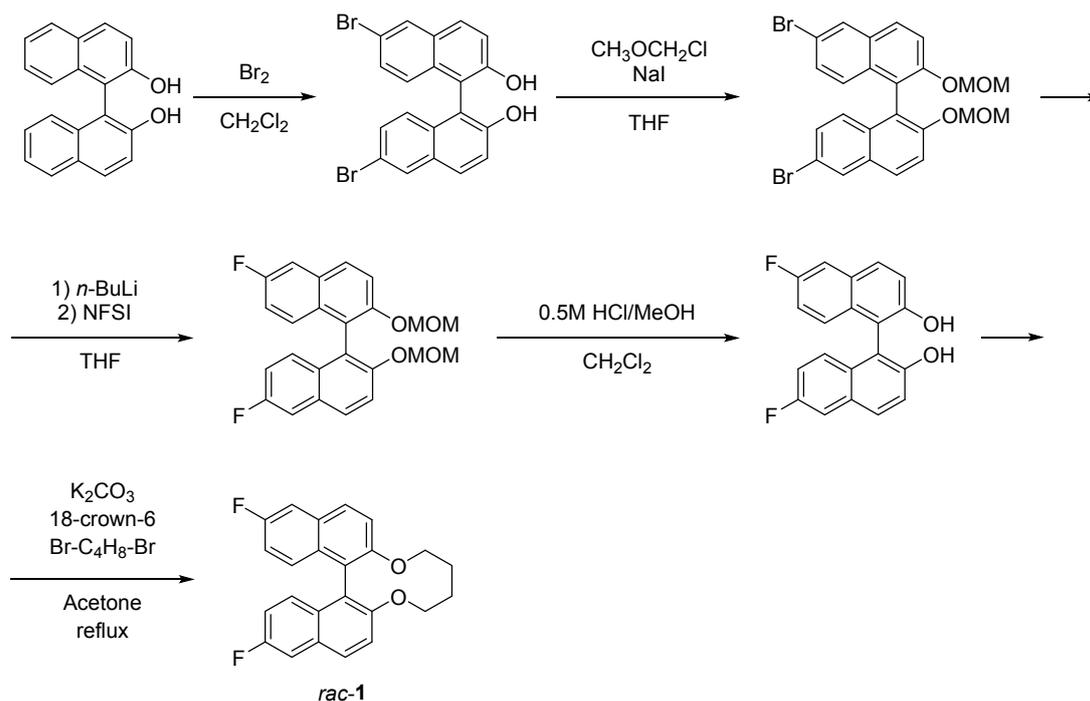
Scheme S1 Synthetic route of *rac*-**1.**

1.3 Chemical Structure of Materials
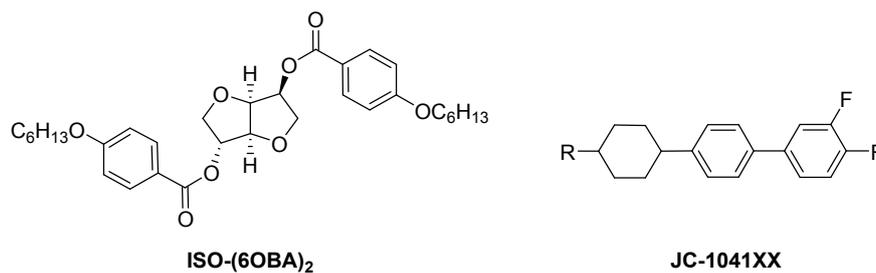
ISO-(6OBA)₂   **JC-1041XX**

Fig. S1 The chemical structures of the conventional chiral dopant ISO-(6OBA)₂ and host nematic JC-1041XX.

1.4 Elastic Constants[4]

Each sample was filled into ITO coated sandwiched-glass cells (cell gap d = 10 μm). The electric fields were applied in the direction perpendicular to the substrate surface. For the applied electric field to measure voltage dependency of the electric capacitance, a small sine wave alternate current (AC) field with 1kH frequency was imposed to a square wave AC field with 10 Hz frequency. The electric capacitance was evaluated by the small sine wave of AC field at 1 kHz, and the nematic director was reoriented by the square wave of AC field at 10 Hz. The applied voltage of square wave of AC field at 10 Hz was increased in 0.1 V step from 0 to 15 V. A threshold voltage (V_{th}) and a dielectric constant anisotropy ($\Delta\varepsilon$) were

determined with capacitance method using a capacitance-voltage (*C-V*) measurement system (Toyo Co.).The elastic constant K_{11} derived from the following equation;

$$V_{th} = \pi \sqrt{\frac{K_{11}}{\varepsilon_0 |\Delta\varepsilon|}}$$

where ε_0 is a vacuum permittivity. The *C-V* curves were fitted to the equation to approximate the elastic constants K_{33}

$$\frac{C}{C_0} = \frac{2}{\pi} \sqrt{1 + \gamma sin^2\theta_m} \frac{V_{th}}{V} \int_0^{\theta_m} \sqrt{\frac{(1 + \gamma sin^2\theta)(1 + \kappa sin^2\theta)}{sin^2\theta_m + sin^2\theta}} d\theta$$

$$\kappa = \frac{K_{33} - K_{11}}{K_{11}}$$

$$\gamma = \frac{\varepsilon_{\parallel} - \varepsilon_{\perp}}{\varepsilon_{\parallel}}$$

where C_0 is initial capacitance, γ is the normalized dielectric constant, κ is the elastic constant ratio, and θ_m is the tilt angle at *d/2* depth. The fitting of *C-V* curves was performed by matching the fitting parameter χ^2 distribution for samples 3 and 4, χ^2 and other parameters are shown in following section.

1.5 Electro-optical Properties

   Using experimental setup for electro-optical properties of blue phases, the Kerr constant and response times is determined as below;

$$\Delta n = \lambda K E^2$$

$$\Delta n = \frac{\lambda}{\pi d} Sin^{-1} \sqrt{\frac{I}{I_0}}$$

where Δn is an electric-field-induced birefringence of the blue phase, λ is a wavelength of the He-Ne Laser, K is the Kerr constant, E is an applied electric field to the blue phase, d is a thickness of the glass cell and I/I_0 is a transmittance of the blue phase with the applied electric field. The Kerr constant was evaluated by a slope of the plotting Δn against E^2.

   Response times of the blue phase were estimated by a τ_{rise} (10 – 90% transmittance change) and a τ_{decay} (90 – 10% transmittance change) at the time of voltage applied and removal, respectively.

He-Ne LASER (633 nm)
JDS Uniphase 1103P

Polarizer

Temp. controller
Linkam 10013L

Quarter wave plate

Digital multimeter
APC Corp. 7461A

Polarizer

Glass cell
with comb type electrodes
(cell gap = ca. 10 μm)

Pinhole

Amplifier
TOYO Corp. HVA-400

Function generator
NF Corp. WF1974

Comb type electrodes (Cr)

Pinhole

4 μm

Analizer

Oscilloscope
LeCroy Waver runner 64Xi

10 μm

Photo detector
New Focus Inc. 1621

Fig. S2 Experimental setup for electro-optical properties of blue phases.

2. Experimental Data

2.1 Phase Transition Behavior

2.1.1 Polarizing Optical Microscopy Images of Sample 1 (ISO-(6OBA)$_2$)

(a)

(b)

(c)

(d)
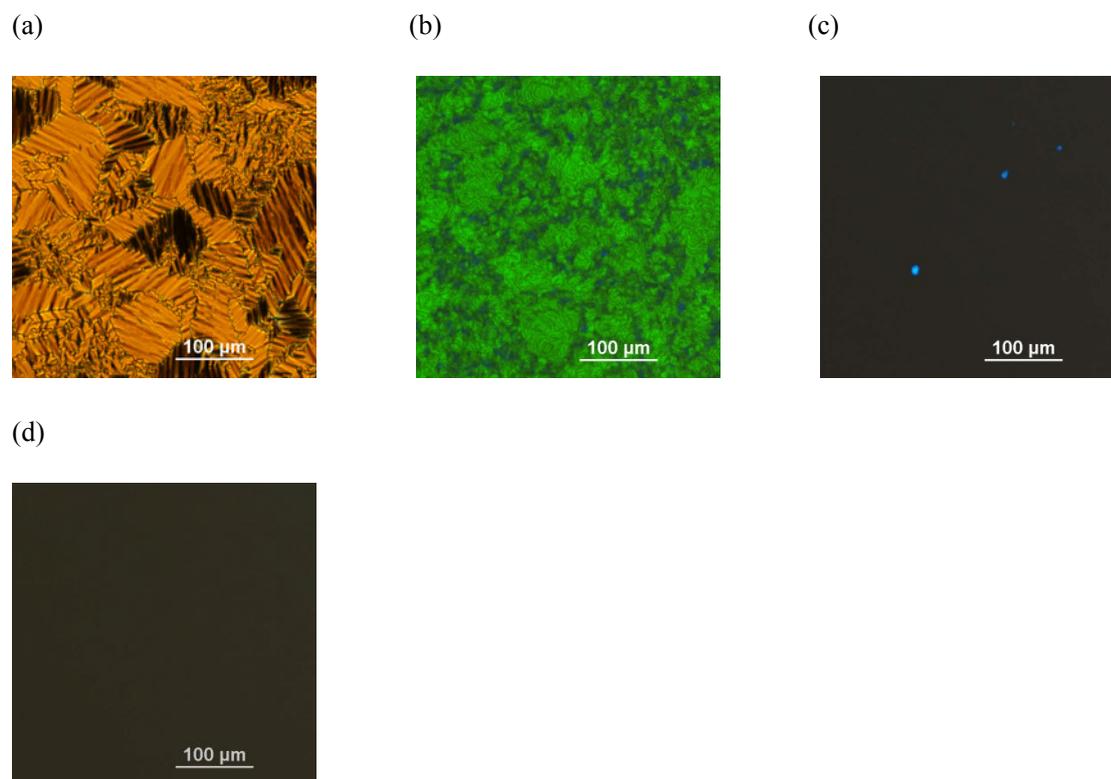
Fig. S3 Polarizing optical microscopy images of the sample 1. (a) focal conic texture of chiral nematic phase at 77.2 °C, (b) platelet texture of blue phase I at 78.0 °C, (c) platelet texture of blue phase II at 78.3 °C, and (d) dark field of isotropic phase at 79.5 °C.

(a)

(b)

(c)

(d)

(e)
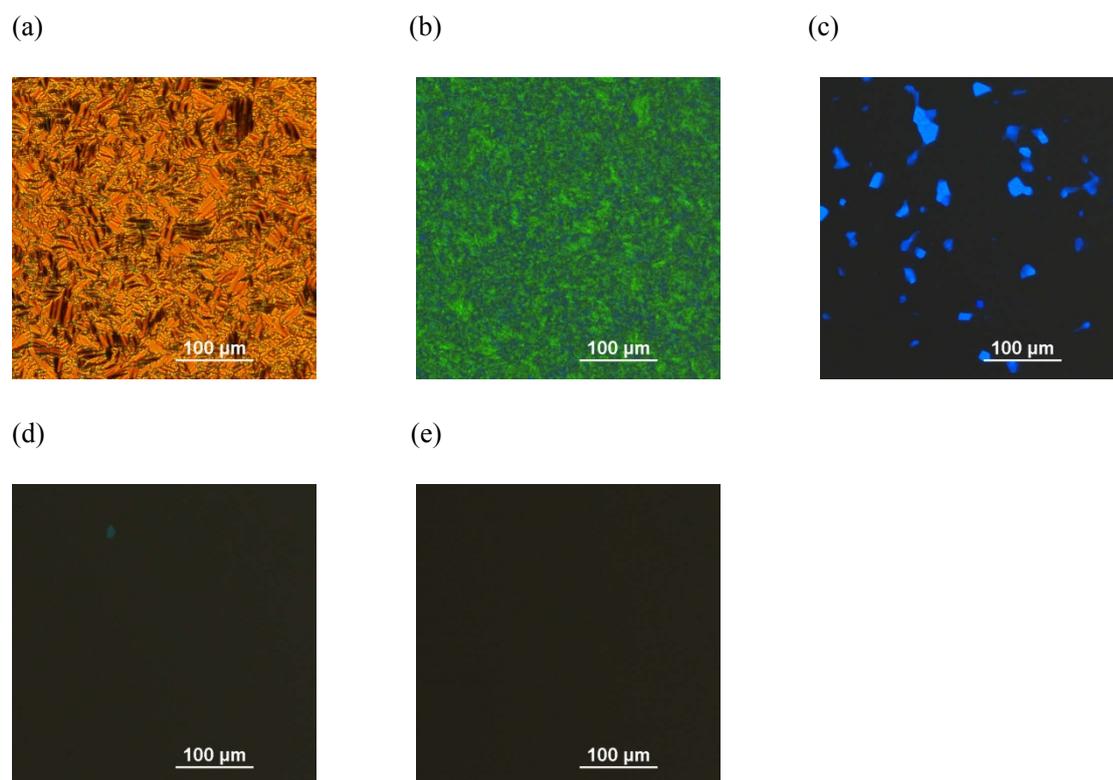
Fig. S4 Polarizing optical microscopy images of the sample 2. (a) focal conic texture of chiral nematic phase at 59.5 °C, (b) platelet texture of blue phase I at 60.6 °C, (c) platelet texture of blue phase II at 62.2 °C, (d) platelet texture of blue phase II at 64.6 °C, and (e) dark field of isotropic phase at 66.1 °C.

(a)

(b)

(c)

(d)

(e)

(f)

Fig. S5 Polarizing optical microscopy images of the sample 4. (a) uniform texture of nematic phase at 55.2 °C, (b) schlieren texture of nematic at 55.2 °C (non-alignment area), (c) uniform texture of nematic phase at 59.3 °C, (d) nematic + isotropic phase at 61.7 °C, (e) nematic + isotropic phase at 63.5 °C, and (f) dark field isotropic phase at 66.0 °C.

2.2 Measurement of Elastic Constants

2.2.2 Measurement of Elastic Constants of Sample 3 (without chiral dopant)

Table S1 Temperature dependences of elastic constants and other parameters of sample 3. The reduced temperature $T - T_c$ represents the temperature difference from the clearing point, $\Delta\varepsilon$ is dielectric anisotropy, V_{th} is threshold voltage of a nematic phase, γ and κ are fitting parameters, χ^2 is chi-square distribution, K_{11} and K_{33} are elastic constants, and K_{33}/K_{11} is elastic constant ratio.

				JC-1041XX / *rac*-1 = 100 / 0 (Sample 3)				
$T - T_c$ / °C	$\Delta\varepsilon$	V_{th} / V	γ	κ	χ^2 / 10^{-5}	K_{11} / pN	K_{33} / pN	K_{33}/K_{11}
-5	3.378	1.104	0.782	1.386	10.877	3.695	8.805	2.385
-4	3.243	1.102	0.742	1.223	9.550	3.534	7.840	2.223
-3	3.102	1.073	0.703	1.317	8.829	3.202	7.395	2.317
-2	2.929	1.051	0.658	1.307	6.301	2.902	6.692	2.307
-1	2.697	1.043	0.596	1.093	5.838	2.631	5.828	2.215

2.2.3 Measurement of Elastic Constants of Sample 4 (rac-1)

Table S2 Temperature dependences of elastic constants and other parameters of sample 4. The reduced temperature $T - T_c$ represents the temperature difference from the nematic-coexisting phase transition temperature, $\Delta\varepsilon$ is dielectric anisotropy, V_{th} is threshold voltage of the nematic phase, γ and κ are fitting parameters, χ^2 is chi-square distribution, K_{11} and K_{33} are elastic constants, and K_{33}/K_{11} is elastic constant ratio.

JC-1041XX / rac-1 = 91.5 / 8.5 (Sample 4)								
$T - T_c$ / °C	$\Delta\varepsilon$	V_{th} / V	γ	κ	χ^2 / 10^{-5}	K_{11} / pN	K_{33} / pN	K_{33}/K_{11}
-5	3.477	0.932	0.688	0.866	4.131	2.712	5.056	1.865
-4	3.357	0.920	0.659	0.890	5.330	2.551	4.818	1.889
-3	3.206	0.908	0.622	0.928	4.670	2.371	4.567	1.926
-2	3.061	0.887	0.591	0.959	3.871	2.146	4.226	1.969
-1	2.878	0.869	0.553	0.910	3.493	1.951	3.727	1.910

2.3 Measurement of Electro-optical Properties

2.3.1 Electro-optical Properties of Sample 1 (ISO-(6OBA)₂)
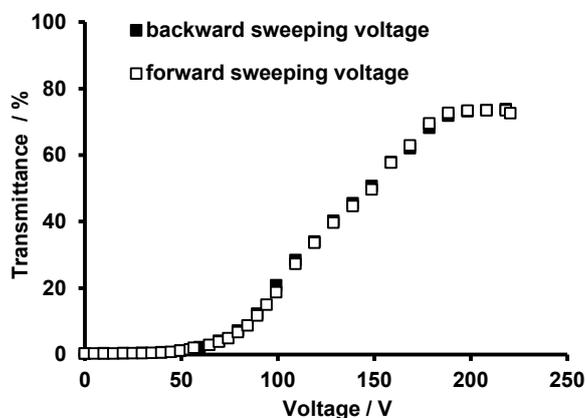
Fig. S6 Voltage-Transmittance curves of Sample 1.
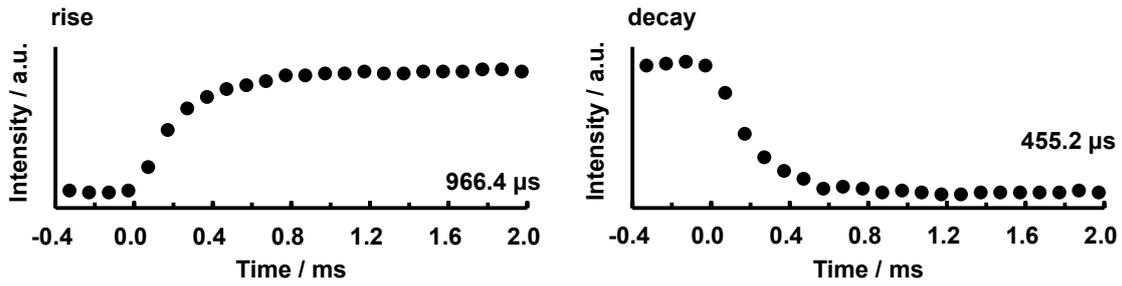
Fig. S7 Response times of sample 1.

*2.3.2 Electro-optical Properties of Sample 2 ((R)-**1**)*
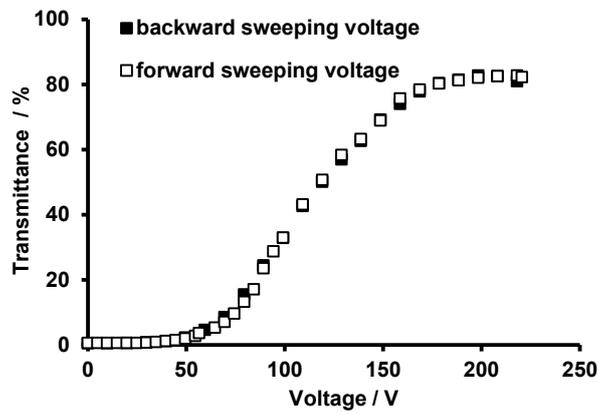
Fig. S8 Voltage-Transmittance curves of Sample 2.
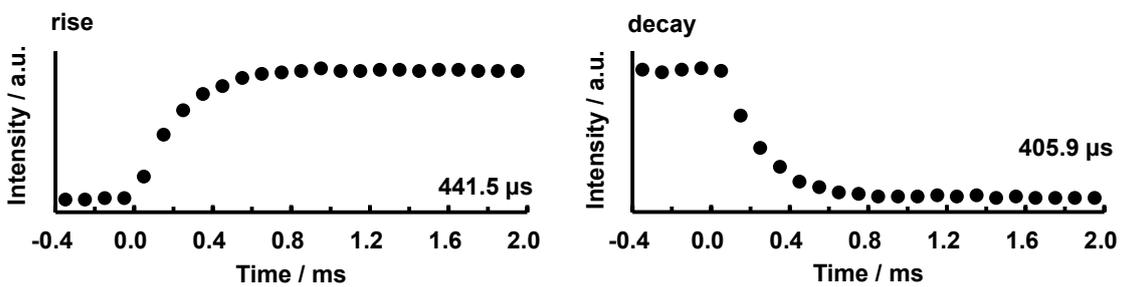
Fig. S9 Response times of sample 2.

3. References

1   H. Ishitani, M. Ueno and S. Kobayashi, *J. Am. Chem. Soc.* 2000, **122**, 8180-8186.

2   T. Mori, M. Kyotani and K. Akagi, *Macromolecules*, 2008, **41**, 607-613.

3   K. Kakisaka, H. Higuchi, Y. Okumura and H. Kikuchi, *Chem. Lett.* 2014, **43**, 624–625.

4   S. Shibayama, H. Higuchi, Y. Okumura and H. Kikuchi, *Adv. Funct. Mater.*, 2013, **23**, 2387-2396.